ACTA ENTOMOLOGICA
MUSEI NATIONALIS PRAGAE
ISSN 1804-6487 (online) – 0374-1036 (print)

2019
59(1): 217–228
doi: 10.2478/aemnp-2019-0019
www.aemnp.eu

RESEARCH PAPER

The first hygropetric *Platynectes* and its larva from eastern China (Coleoptera: Dytiscidae)

Jiří HÁJEK[1)], Yves ALARIE[2)], Jaroslav ŠŤASTNÝ[3)] & Dominik VONDRÁČEK[1)]

[1)] Department of Entomology, National Museum, Cirkusová 1740, CZ-193 00 Praha 9 – Horní Počernice, Czech Republic; e-mails: jiri_hajek@nm.cz; dominik.vondracek@gmail.com
[2)] Department of Biology, Laurentian University, Sudbury, ON P3E 2C6, Canada; e-mail: yalarie@laurentian.ca
[3)] Kosmonautů 359, CZ-460 05 Liberec, Czech Republic; e-mail: jaroslav.stastny@jergym.cz

Accepted:
30th May 2019

Published online:
20th June 2019

Abstract. *Platynectes* (*Gueorguievtes*) *davidorum* sp. nov. is described, including all larval instars, from hygropetric habitats in Fujian and Zhejiang provinces, eastern China. The new species can be easily distinguished from all other Asia *Platynectes* Régimbart, 1879 with dorsally strongly convex habitus, distinctly impressed double reticulation of elytra, short appendages and the shape of median lobe of aedeagus. Collected larvae were successfully associated with adults using a molecular approach and the barcode for the new species is provided as well as the phylogenetic position based on the mitochondrial cytochrome oxidase I gene; they are described and illustrated, with detailed morphometric and chaetotaxic analyses of the cephalic capsule, head appendages, legs, last abdominal segment, and urogomphi. The classification of the new species within the subgenus *Gueorguievtes* Vazirani, 1976, and its adaptation to hygropetric habitats are briefly discussed.

Key words. Coleoptera, Dytiscidae, *Platynectes*, taxonomy, phylogeny, cytochrome oxidase I, barcode, new species, larva, chaetotaxy, hygropetric habitat, China, Palaearctic Region

Zoobank: http://zoobank.org/urn:lsid:zoobank.org:pub:A54B960F-7C0D-4CC5-9111-83EAA9A5BD74

Introduction

The agabine genus *Platynectes* Régimbart, 1879 includes 67 species occurring in Australian, Neotropical, Oriental and Palearctic Regions. The first attempt of *Platynectes* classification was made by Guéorguiev (1972), later revised by Vazirani (1976) and Guéorguiev (1978), who recognized four to five subgenera based on characters on prosternal process, metacoxal lines and male genitalia. Ribera et al. (2008) showed *Platynectes* to be paraphyletic, with the Australian species resolved as sister to *Agametrus* Sharp, 1882 and *Leuronectes* Sharp, 1882 and the Neotropical species forming a clade with *Hydrotrupes* Sharp, 1882 and the Laccophilinae genus *Agabetes* Crotch, 1873. Recently, Toussaint et al. (2017), in a molecular phylogenetic analysis, confirmed the paraphyly of *Platynectes* with respect to *Leuronectes* and *Agametrus*. They relegated *Agametrus* as a subgenus of *Platynectes* and included in it the species previously assigned to *Leuronectes*. These authors also included *Platynectes* in its own tribe Platynectini, a placement supported by Michat et al. (2017) based on larval characters. Formally, *Platynectes* is currently divided into four subgenera: Cordilleran *Agametrus*, monotypic Australian *Australonectes* Guéorguiev, 1972, Palaearctic, Oriental and Australian *Gueorguievtes* Vazirani, 1976 and Neotropical *Platynectes* s. str. (cf. Nilsson & Hájek 2019).

At the present time, larvae of only three species of *Platynectes* have been described: the mature larva of Australian *P. decempunctatus* (Fabricius, 1775) superficially described several years ago (Watts 1963, Bertrand 1972), and more recently the larvae of Neotropical *P. curtulus* (Régimbart, 1899) (as *Leuronectes*) (Michat & Archangelsky 2009) and *P. decemnotatus* (Aubé, 1838) (Benetti et al. 2019) both of which according to the now generalized larval descriptive format of Hydradephaga, which incorporates chaetotaxic analysis.

Nine *Platynectes* species are currently known from China (Nilsson 1998, Šťastný 2003). Recent collecting efforts of the senior author in eastern China revealed presence of another peculiar *Platynectes* species presumably

inhabiting hygropetric habitats exclusively. Its formal description, including description of its larva is the aim of the present paper.

Material and methods

Molecular analysis. For the association of larvae with adults, and for the phylogenetic position of the new species within *Platynectes*, DNA sequences of the 3′ region of the mitochondrial cytochrome oxidase I gene (cox1) were obtained. One male, one female and two larvae of instar III of *Platynectes davidorum* sp. nov. were used. We also extracted the only specimen of different species (*Platynectes dissimilis* (Sharp, 1873)) from the same collecting event. In addition, the 5′ (barcode) region of the cox1 is provided for female paratype and available on the Barcode of Life Data Systems (BOLD; Ratnasingham & Hebert 2007) under the specific process ID (see type material); this sequence was however not used in the analysis. Other already existing sequences of *Gueorguievtes* species were downloaded from GenBank and added to the analysed dataset. As an outgroup, several Australian and American taxa of the genus *Platynectes* were chosen.

For details about the laboratory protocols follow Vondráček et al. (2018b) including primers and PCR protocol for the barcode region. For the amplification details of the 3′ region of cox1, follow Vondráček et al. (2018a). Obtained sequences of the 3′ region of cox1 were submitted to the GenBank (NCBI) under accession numbers (see Fig. 1). Methods used for the editing and the subsequent analyses of obtained sequences are described in detail in Šumpich & Jaroš (2019). The only difference was in the number of generations during the Bayesian inference computational method, which was set to 20×10^6 in this study.

Adult morphology. The material was examined using an Olympus SZX12 stereomicroscope. Habitus photograph were taken using a Canon EOS 550D digital camera with an attached Canon MP-E65mm f/2.8 1–5× macro lens as numerous separate images at different focal planes and afterwards combined using Helicon Focus 6.3.0 software. The male genitalia were studied and illustrated in temporary glycerine mounts using an Olympus BX41 transmitted light microscope with Canon DS126291 attachment; they were subsequently washed in distilled water and mounted in DMHF on the same card as the beetle.

Measurements were taken with an ocular graticule. The following abbreviations were used in the descriptions:

MW maximum width of body;
TL total length of body, a single measurement of length from front of head to apex of elytra;
TL-h total length without head length, length of body from anterior margin of pronotum to apex of elytra;
WC/WS ratio of width of metacoxa (WC) along extension of line in maximum width of metaventrite (WS) at the point of closest approximation of metacoxa to mesocoxal cavity (cf. Petrov et al. 2010: 43, Fig. 3).

The terminology to denote the orientation of the genitalia follows Miller & Nilsson (2003).

Larval morphology. Habitus photograph of larva in alcohol was taken in the same way as that of the adult. Larvae were disarticulated and mounted on standard glass slides in Hoyer's medium. Microscopic examination at magnifications of 80–800× was done using an Olympus BX50 compound microscope equipped with Nomarsky differential interference optics. Figures were prepared through use of a drawing tube attached to the microscope. Drawings were scanned and digitally inked using an Intuos 4 professional pen tablet (Wacom Co., Ltd. Kazo, Saitama, Japan).

All measurements were made with a compound microscope equipped with a micrometer eyepiece. The part to be measured was adjusted so that it was, as nearly as possible, parallel to the plane of the objectives. We employed, with minimal modifications and additions, the terms used in previous papers dealing with larval morphology of Agabinae (Alarie & Larson 1998; Alarie et al. 1998, 2019; Michat & Archangelsky 2009; Benetti et al. 2019). The following measurements were taken (with abbreviations in parentheses).

A length of antenna;
A3' apical lateroventral process of the third antennomere;
CL length of the longest claw on the respective leg;
COL coronal line length;
FRL length of frontoclypeus; total length from apex of nasale to posterior margin of ecdysial suture;
HL head length; total head length including the frontoclypeus, measured medially along the epicranial stem;
HW maximum head width;
MNL length of mandible; measured from laterobasal angle to apex;
MNW width of mandible; maximum width measured at base.
MP length of maxillary palpi;
L length of leg; including the longest claw (CL);
LP length of labial palpi;
OCW occipital foramen width; maximum width measured along dorsal margin of occipital foramen);
U length of urogomphus.

Length of antenna (A), maxillary (MP) and labial (LP) palpi were derived by adding the lengths of the individual segments; each segment is denoted by the corresponding letter(s) followed by a number (e.g., A1 – first antennomere). Length of leg (L), including the longest claw (CL), was derived by adding the lengths of the individual segments; each leg is denoted by the letter L followed by a number (e.g., L1 – prothoracic leg). The length of trochanter includes only the proximal portion, the length of distal portion is included in the femoral length. The legs were considered as being composed of six segments following Lawrence (1991). Dorsal length of last abdominal segment (LAS) – measured along midline from anterior to posterior margin. Length of urogomphus (U) was derived by adding the lengths of the individual segments; each segment is denoted by the letter U followed by a number (e.g., U1 – first urogomphomere). These measurements were used to calculate several ratios that characterize body shape.

Description of colour is given from ethanol-preserved specimens.

Chaetotaxic analysis. Primary (present in first-instar larva) and secondary (added in later instars) setae and

so-called pores were distinguished in the cephalic capsule, head appendages, legs, last abdominal segment and urogomphus. Sensilla were coded by two capital letters, in most cases corresponding to the first two letters of the name of the structure on which are located, and a number (setae) or a lower case letter (pores). The following abbreviations were used:

AB abdominal segment VIII;
AN antenna;
CO coxa;
FE femur;
FR frontoclypeus;
LA labium;
MN mandible;
MX maxilla;
PA parietal;
PT pretarsus;
TA tarsus;
TI tibia;
TR trochanter;
UR urogomphus.

Setae and pores present in first-instar larva were labelled by comparison with the ground-plan of chaetotaxy of the subfamilies Agabinae and Colymbetinae (Alarie 1995, 1998). Homologies were recognized using the criterion of similarity of position (Remane 1952). Setae located at the apices of the maxillary and labial palpi were extremely difficult to distinguish due to their position and small size. Accordingly, they are not well represented in the drawings. The number of secondary setae present on the anteroventral (AV) margin of femur was more difficult to assess owing to the presence of a variable number of additional primary setae. To solve that problem, the following rule was applied: number of AV secondary setae on femur = total number of setae over anterior surface - [number of primary setae (= 6, seta FE1 excluded) + maximum number of additional setae recorded (2 or 3 depending on which leg is studied)].

Material examined. Exact label data are cited and given in quotation marks for the type material. Authors' additional remarks are provided in square brackets; [p] – preceding data are printed. Separate label lines are indicated by a slash (/), separate labels by a double slash (//).

The specimens included in this study are deposited in the following collections:

IZCAS Institute of Zoology, Chinese Academy of Sciences, Beijing, China;
JSCL Jaroslav Šťastný private collection, Liberec, Czech Republic;
NMPC National Museum, Prague, Czech Republic;
SNUC Shanghai Normal University, Shanghai;
YALC Yves Alarie Larval Collection, Department of Biology, Laurentian University, Sudbury, Canada.

Results of molecular analysis

All four samples of *Platynectes davidorum* sp. nov. resulted as very close relatives to each other in one clade (see Fig. 1), which is fully supported (posterior probability = 1.00). The average genetic distance between these four samples is 0.33%, which confirms that the larvae and adults are members of the same species. Our female sample of *Platynectes dissimillis* from the same cliff, and downloaded sequences of *P. gemellatus* Šťastný, 2003 resulted as sister species forming a clade sister to *P. davidorum* sp. nov., but with very low posterior probability between the split of these two clades (Fig. 1). The average genetic distances between *P. davidorum* sp. nov., *P. dissimillis* and *P. gemellatus* are: *dissimilis* × *davidorum* = 13.1%, *gemellatus* × *davidorum* = 12.5% , *dissimilis* × *gemellatus* = 3.3%.

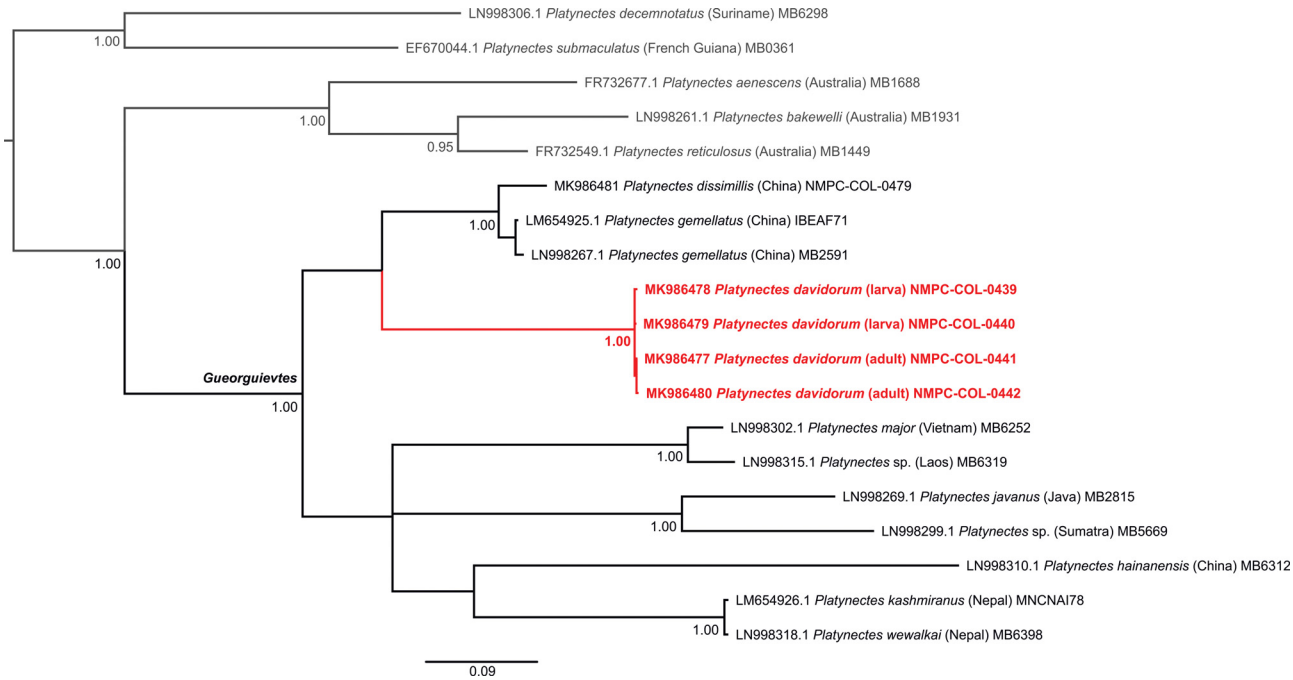

Fig. 1. Majority-rule consensus tree from Bayesian analysis based on the 3′ region of the cytochrome oxidase I gene of the subgenus *Gueorguievtes* and several outgroup taxa (in grey) of the genus *Platynectes*. Posterior probabilities are provided only for splits indicating 0.95 or higher probability. Tip labels include (from left to right) GenBank accession number, taxon name, country of origin, and the DNA voucher label.

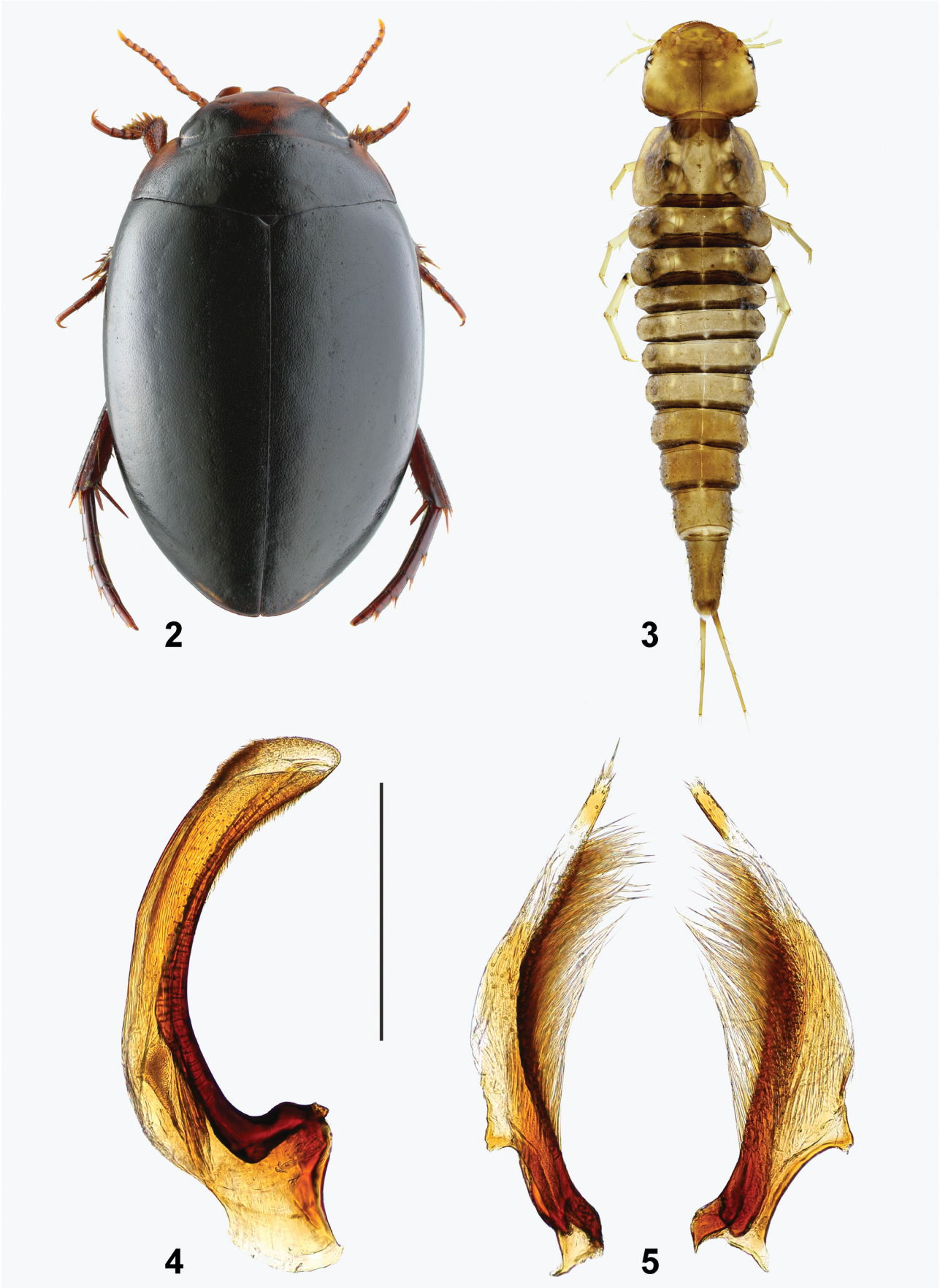

Figs 2–5. *Platynectes davidorum* sp. nov. 2 – habitus of ♂ paratype (5.1 mm); 3 – 3rd instar larva (6.6 mm); 4 – median lobe of aedeagus in lateral view; 5 – parameres. Scale bar = 0.5 mm (Figs 4–5).

Taxonomy

Platynectes (*Gueorguievtes*) *davidorum* sp. nov.

(Figs 2–23, 26)

Type locality. China, Fujian Province, Nanping Prefecture, Wuyishan Mountains, Tongmu – Sangang village, ca. 27°45.0′N, 117°40.7′E.

Type material. Holotype: ♂ (IZCAS), labelled: '**CHINA:** Fujian prov., 23.v.-3.vi.2018 / Wuyishan Mts. NNR, **Sangang** vill. env. / 27°45.0′N, 117°40.7′E, 720 m / river valley; wet rock along road / J.Hájek, D.Král, J.Růžička & L.Sekerka lgt. // NMPC-COL-442 [DNA voucher number; p] // HOLOTYPE ♂ / *PLATYNECTES* / *davidorum* sp. nov. / J. Hájek et al. det. 2019 [p, red label]'. Paratypes: 4 ♂♂ 5 ♀♀, same label data as holotype (JSCL, NMPC); 1 ♀, same label data as holotype but with additional label 'NMPC-COL-441 [DNA voucher number; p] / BOLD DNMPC572-19 [BOLD Process ID]' (NMPC); 1 ♀, same label data as holotype, but 'Yandong Chen lgt. [p]' (IZCAS); 1 ♀, labelled: '**CHINA:** Fujian prov., 23.v.-3.vi.2018 / Wuyishan Mts. NNR, **Sangang** vill. / 27°45.0′N, 117°40.7′E, 720 m / river valley, mixed forest+bamboo; at light / J.Hájek, D.Král, J.Růžička & L.Sekerka lgt. (NMPC); 1 ♀ 'Mt. Yandangshan / Wenzhou City / Zhejiang Prov. / alt. 150-350m / 30-V-2006 / LI & SHEN leg. [p]' (SNUC). All paratypes with the respective red printed label.

Material of larvae. 1 larva of instar I, 2 larvae of instar II and 5 larvae of instar III, same locality data as holotype (NMPC, YALC). Two larvae of instar III with additional label 'NMPC-COL-439 [DNA voucher number; p]', NMPC-COL-440 [DNA voucher number; p]'.

Description of adult. ***Male holotype.*** *Habitus* (Fig. 2) elongate oblong oval, distinctly convex with continuous outline, broadest before elytral midlength, dorsally convex. Dorsal surface submatt due to distinct reticulation.

Colouration. Dorsal surface black with orange-reddish marking: head with pale clypeus, large triangular spot on frons between eyes and two oval spots on vertex; pronotum with pale anterior corners and indistinctly translucent anterior margin; elytra with indistinct pale lateral band beginning after elytral midlength, shortly interrupted subapically, and with small preapical spot. Ventral surface black with reddish-brown basal half of epipleura and indistinct spots laterally on abdominal ventrites. Appendages reddish-brown.

Head. Moderately broad, ca. 0.65× width of pronotum, transversely elliptical. Anterior margin of clypeus truncate. Antennae with antennomeres rather broad, only slightly longer than wide; club-shaped. Eyes emarginate anterolaterally. Punctation double; several large setigerous punctures present in fronto-clypeal grooves and in depressions along inner margin of eyes; fine punctures distributed sparsely and irregularly on head surface, mostly in intersections of reticulation. Reticulation deeply incised consisting of heterogeneous, longitudinally somewhat elongated, polygonal meshes; meshes mostly closed, usually with several micropunctures inside. Microreticulation present only on vertex posterior to eyes.

Pronotum. Transverse, broadest at posterior angles. Anterior angles acute, posterior angles obtusely rectangular. Sides slightly and evenly curved, with distinct lateral beading. Anterior margin straight (dorso-frontal view), posterior margin slightly sinuate. Punctation double, similar to that of head; row of coarse setigerous punctures present along anterior and basal margin (except for medially); fine punctures distributed irregularly on pronotal surface, presenting mostly in intersections of reticulation. Reticulation similar to that of head, consisting of heterogeneous polygonal meshes; meshes sometimes not closed (especially on disc), usually with several micropunctures inside; meshes larger and less impressed on disc, becoming much smaller and deeply impressed near sides. Microreticulation barely perceptible, occurring only near sides. Centre of pronotal disc with small indistinct longitudinal furrow.

Scutellar shield broadly triangular.

Elytra broadest at midlength, sides evenly rounded, lateral margin distinctly bordered. Punctation double; coarse punctures present in two relatively distinct longitudinal discal lines and irregular lateral line, few punctures present also along suture; fine punctures distributed irregularly over elytral surface, occurring mostly in intersections of reticulation. Reticulation well impressed, similar to that of head and pronotum, consisting of heterogeneous polygonal meshes; meshes sometimes not closed, usually with several micropunctures inside. Microreticulation weakly impressed, more apparent laterally and apically, consisting of heterogeneous polygonal meshes.

Legs. Meso- and metafemora with bunch of spiniform setae along posterolateral margin. Pro- and mesotibia widened, club shaped, densely punctured with spinigerous punctures over ventral surface. Metatibia with two lines of coarse spinigerous punctures over ventral surface. Pro- and mesotarsomeres 1–3 moderately dilated, ventrally with adhesive setae. Metatarsal claws subequal; anterior (lateral) claw slightly shorter than posterior (medial) one. Surface of legs with distinct reticulation consisting of elongate oblique or transverse meshes. Elongate natatorial setae present along dorsal margin of all tibiae and pro- and mesotarsomeres (although in a lesser number), and along both dorsal and ventral margins (especially dorsal margin) of metatarsomeres.

Ventral surface. Genae reticulated with transverse meshes. Prosternum sinuate anteriorly, obtusely keeled medially. Lateral portions of prosternum with transverse reticulation. Prosternal column shiny, with sparse double punctation; slopes of prosternal column densely and coarsely punctate. Prosternal process shortly lanceolate, in cross-section slightly convex; distinctly bordered in basal half, apex pointed; surface with irregular sparse double punctation. Medial part of metaventrite without microsculpture, shiny, with sparse fine punctation; lateral parts of metaventrite ('metasternal wings') slender, tongue-shaped, transversely reticulated. Ratio WC/WS = 4.1. Metacoxal lines well impressed, incomplete anteriorly, almost parallel-sided. Metacoxal plates reticulated with polygonal meshes, punctation consisting of sparse fine punctures. Abdominal ventrites I–V with reticulation consisting of longitudinal (I), oblique (II) or transverse (III–V) meshes; ventrites III–V additionally with numerous fine transverse wrinkles medially. Punctation double; bunch of coarse setigerous punctures present in centre of ventrites III–V, additional setigerous punctures arranged sparsely in transverse line in medial part of ventrites; fine punctures distributed sparsely and irregularly on ventrite surface, predominantly on border lines of meshes of reticulation. Apical abdominal ventrite (VI) with posterior margin regularly rounded, distinctly beaded; reticulation present only baso-laterally;

surface of disc with fine transverse wrinkles; with short and deep longitudinal grooves along posterior margin; punctation double, coarsely punctured along posterior margin, sparsely and finely punctured on disc.

Male genitalia. Median lobe (Fig. 4) in lateral aspect simple, sickle-shaped, distinctly setated subapically along both ventral and dorsal margins; apex slightly broadened, asymmetrical. Parameres (Fig. 5) slender, densely setated dorsally, with a distinct subbasal tooth on ventral side; left paramere more slender than the right one.

Female differs from male in the following characters: meshes of dorsal surface reticulation more deeply engraved and longitudinally stretched, surface appearing more matt, interstices more densely punctate; abdominal ventrite VI with sublateral rugose area large, punctures confluent, forming several longitudinal grooves, medially not rugose and densely punctate; pro- and mesotibia less widened; pro- and mesotarsomeres 1–3 not dilated and without adhesive setae.

Measurements (N = 14). TL: 4.9–5.4 mm (mean value: 5.1 ± 0.2 mm); holotype: 5.0 mm. Tl-h: 4.4–4.9 mm (mean value: 4.6 ± 0.2 mm); holotype: 4.5 mm. MW: 3.0–3.3 mm (mean value: 3.1 ± 0.1 mm); holotype: 3.0 mm.

Description of larva. Instar I (Figs 6–18). Body subcylindrical, narrowing towards abdominal apex. Measurements and ratios that characterize the body shape are shown in Table 1. Body colour predominantly piceous to grey; head capsule with two yellowish maculae mesally; head appendages predominantly creamy white to pale yellow; thoracic and abdominal terga grey; legs predominantly creamy white with some greyish maculae; urogomphus yellow except over proximal 1/3 piceous to grey.

Head. Cephalic capsule (Figs 6–7) subquadrate, about as broad as long; maximum width at about level of primary seta PA6; lateral margin of parietale straight; neck constriction present; occipital suture absent; ecdysial line well marked, coronal line long; occipital foramen broadly emarginate ventrally; frontoclypeus rounded mesally, slightly convex, slightly extending medially beyond level of lateral lobes (= adnasalia of Beutel 1994); dorsal surface with two egg bursters (= ruptor ovi of Bertrand 1972), less than half as broad basally than maximum width of antennomere 1; apical margin of frontoclypeus with four spatulate setae (= lamellae clypeales of Bertrand 1972); gular suture visible; ocularium present, with six stemmata subdivided into two vertical series (four stemmata visible dorsally, two ventrally); tentorial pits visible ventrally on each side of middle at about midlength. Antenna (Figs 8–9) elongate, slender, shorter than HW, composed of four antennomeres; A1 and A4 shortest, subequal in length, A2 and A3 subequal in length; A3 with a ventroapical spinula; lateral elongation of antennomere 3 (A3') short and bulge-like. Mandible (Fig. 10) prominent, falciform, longer than broad, distal half projected inwards, apex sharp; mandibular channel present, mesal groove enclosed by two shortly serrate edges; pubescence absent from ventral inner margin. Maxilla (Figs 11–12): cardo small, subovate; stipes short and thick, with minute spinulae along inner margin proximad to galea; galea well developed, subconical; lacinia absent; palpifer short, palpomere-like; palpus elongate, three-segmented, shorter than antenna; MP3 slightly longer than MP2, each longer than MP1. Labium: prementum subrectangular, broader than long; palpus elongate, two-segmented (Fig. 13), subequal to maxillary palpus in length; LP2 subequal in length to LP1.

Thorax. Pronotum trapezoidal dorsally, ovate laterally, shorter than meso- and metanotum combined; meso- and metanotum subequal, with anterotransverse carina; sagittal line visible on three tergites; thoracic sterna membranous; spiracles absent. Legs (Figs 14–15) well developed, robust, composed of six articles (including pretarsus), L3 longest, slightly longer than L1 and L2; CO robust, elongate, TR divided into two parts, trochanteral annulus present; FE, TI and TA slender, subcylindrical; PT with two short and slightly curved claws, posterior claw shorter than anterior claw on L1 and L2, claws subequal in length on L3; ventral margin of protibia and protarsus with elongate spinulae; marginal spinulae more faintly developed on mesotibia and mesotarsus, lacking on L3; comb-like spinulae broadly developed anteroventrodistally on protibia and protarsus.

Abdomen (Figs 16–17) eight-segmented; segments I–VI sclerotized dorsally, membranous ventrally, segment VII with ventral plate distinct from tergite, segment VIII (= LAS) completely sclerotized; all tergites with anterotransverse carina; spiracular openings absent; LAS longest, shortly extended posteriorly, convex medially. Urogomphus (Fig. 18) two-segmented; U1 longer than LAS, much longer than U2.

Chaetotaxy (Figs 6–18). Similar to that of generalized Agabinae larva (Alarie 1995, 1998) except for following features: seta FR5 close to pore FRd; pore ANi minute; A4 with a minute dorso-apical additional pore; pore MXa absent; setae LA10 and LA12 articulated submedially; FE with one anteroventral, one anterodistal and one posteroventral additional setae; seta FE1 inserted proximally; seta FE6 hair-like; seta AB8 minute; despite thorough effort seta AB14 not found on the only specimen available for study; setae UR2, UR3 and UR4 articulated at about mid-length on U1; pore URc located far from apex of U1; U2 with one minute additional seta proximally.

Instar II. As first-instar larva except for the following features: Measurements and ratios that characterize the body shape are shown in Table 1. Head appendages yellowish; legs predominantly yellow to pale brown; urogomphus darker, yellow distally.

Head. Frontoclypeus lacking egg-bursters; apical margin of frontoclypeus with 19 spatulate setae. Antenna with A4 shorter than A1. Maxilla with MP2 subequal to slightly longer than MP1. Labium with LP2 slightly shorter than LP1.

Thorax. L3 longer than L1 and L2.

Abdomen: Segment VII completely sclerotized; siphon slightly emarginated apically; U2 much reduced, considerably shorter than U1.

Chaetotaxy. Cephalic capsule with numerous mostly minute secondary setae; parietale with 6–7 spine-like secondary setae on lateral margin and ventral surface; MN with several minute secondary seta along outer margin,

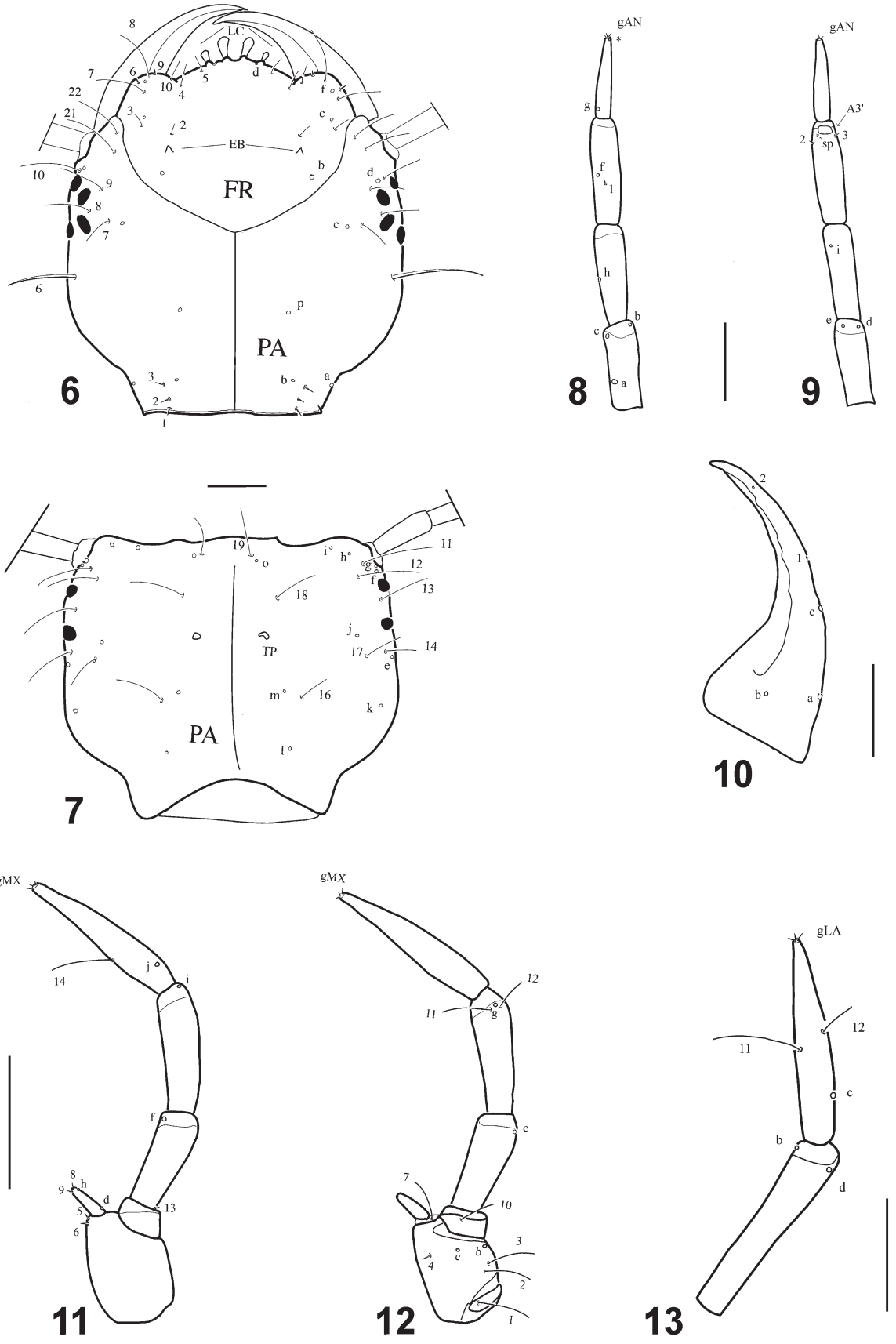

Figs 6–13. *Platynectes davidorum* sp. nov., 1st instar larva. 6 – head capsule, dorsal aspect; 7 – head capsule, ventral aspect; 8 – antenna, dorsal aspect; 9 – antenna, ventral aspect; 10 – mandible, dorsal aspect; 11 – maxilla, dorsal aspect; 12 – maxilla, ventral aspect; 13 – labial palp; dorsal aspect. Abbreviations: EB – egg bursters; FR – frontoclypeus; LC – lamellae clypeales; PA – parietale; sp – spinula, TP – tentorial pits. Numbers and lowercase letters refer to primary setae and pores, respectively. Scale bar = 0.1 mm.

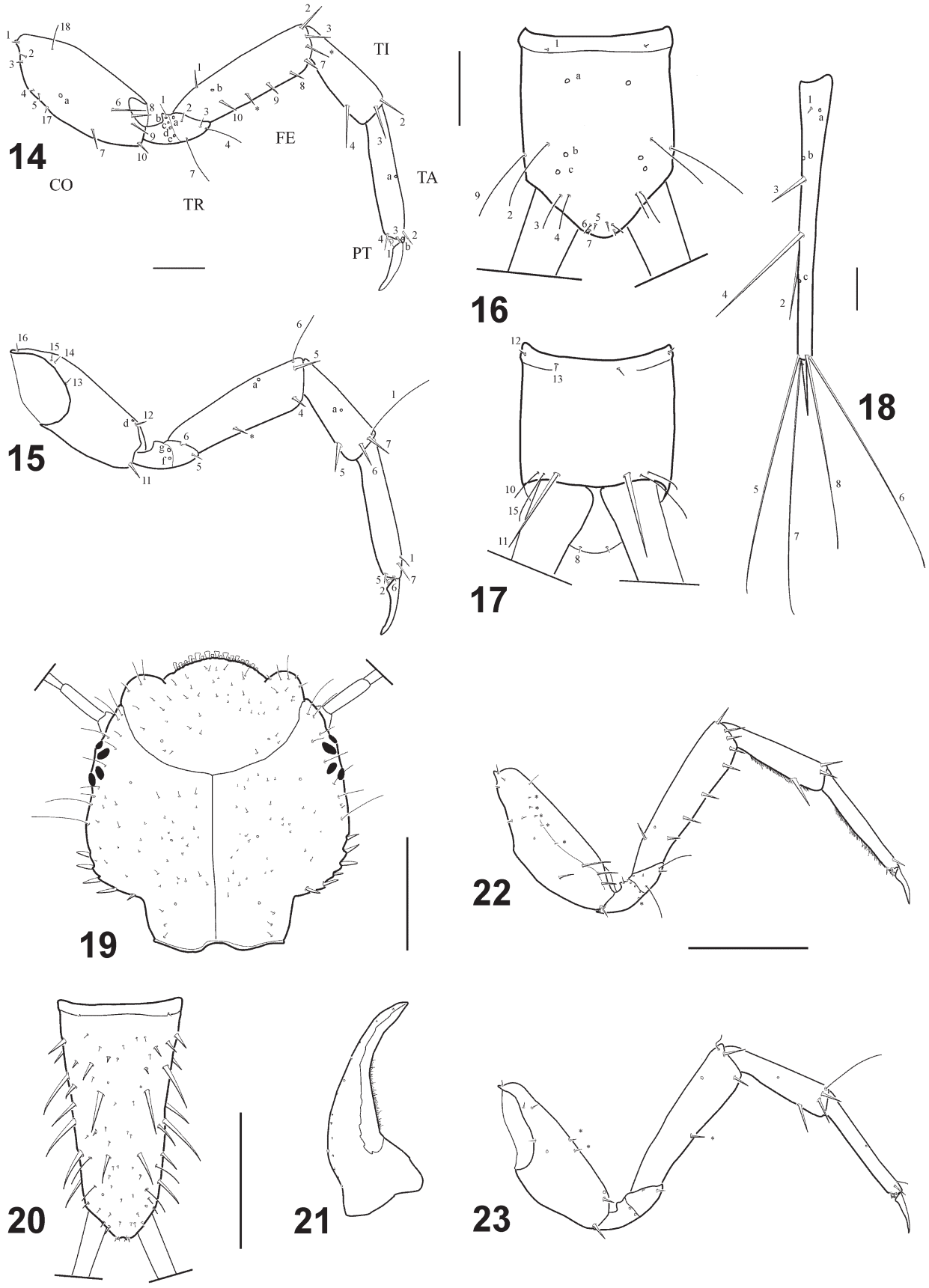

Figs 14–23. *Platynectes davidorum* sp. nov., 1st instar larva (Figs 14–18) and 3rd instar larva (Figs 19–23). 14 – metathoracic leg, anterior surface; 15 – metathoracic leg, posterior surface; 16 – abdominal segment VIII, dorsal aspect; 17 – abdominal segment VIII, ventral aspect; 18 – urogomphus, dorsal aspect; 19 – head capsule, dorsal aspect; 20 – abdominal segment VIII, dorsal aspect; 21 – mandible, dorsal aspect; 22 – metathoracic leg, anterior surface; 23 – metathoracic leg, posterior surface. Abbreviations: CO – coxa; FE – femur; TA – tarsus; PT – pretarsus; TI – tibia; TR – trochanter. Numbers and lowercase letters refer to primary setae and pores, respectively. * = additional (Figs 14–15, 18) or secondary (Figs 22–23) sensilla. Scale bars = 0.1 mm (Figs 14–18) and 0.5 mm (Figs 19–23).

Table 1. Measurements and ratios for the larvae of *Platynectes davidorum* sp. nov.

	Instar I (n = 1)	Instar II (n = 2)	Instar III (n = 3)
HL (mm)	0.63	0.93–0.91	1.28–1.40
HW (mm)	0.60	0.83–0.92	1.20–1.31
FRL (mm)	0.30	0.52–0.54	0.53–0.57
OCW (mm)	0.33	0.40–0.48	0.75–0.82
HL/HW	1.04	1.08–1.12	1.05–1.07
HW/OCW	1.85	1.90–2.10	2.06–2.13
COL/HL	0.52	0.54–0.55	0.58–0.59
FRL/HL	0.48	0.45–0.46	0.41–0.42
A/HW	0.77	0.63–0.71	0.58–0.61
A3/A1	1.29	0.97–1.13	0.80–0.87
A3/A2	1.08	0.94–1.00	0.89–0.93
A3/A4	1.29	1.62–1.66	1.95–2.23
MNL/MNW	2.55	2.46–2.82	2.51–2.80
MNL/HL	0.53	0.48–0.49	0.45–0.49
A/MP	1.30	1.15–1.19	1.20–1.23
GA/MP1	0.42	0.32–0.34	0.31–0.32
PPF/MP1	0.27	0.34–0.35	0.29–0.34
MP2/MP1	1.24	1.03–1.06	0.96–1.00
MP2/MP3	1.00	0.84–0.87	1.05–1.08
MP/LP	0.99	1.11–1.12	1.10–1.11
LP2/LP1	1.02	0.80–0.87	0.65–0.75
L3 (mm)	1.31	2.04–2.18	2.86–3.08
L3/L1	1.08	1.26	1.24–1.27
L3/L2	1.03	1.19	1.15–1.17
L3/HW	2.17	2.37–2.45	2.34–2.39
L3(CO/FE)	1.08	0.98–1.05	1.01–1.03
L3(TI/FE)	0.65	0.67–0.69	0.64–0.65
L3(TA/FE)	0.74	0.76–0.79	0.71–0.73
L3(CL/TA)	0.59	0.38–0.40	0.30–0.36
LAS (mm)	0.27	0.52–0.55	0.87–0.94
LAS/HW	0.45	0.60–0.62	0.64–0.73
U (mm)	0.81	1.04–1.06	1.23–1.38
U1 (mm)	0.66	0.94–0.96	1.18–1.33
U/LAS	2.97	1.91–2.02	1.38–1.46
U1/LAS	2.44	1.73–1.83	1.33–1.41
U/HW	1.34	1.15–1.25	0.97–1.05
U1/HW	1.10	1.04–1.13	0.94–1.02
U1/U2	4.60	9.51–9.70	21.42–26.84

proximal to pore MNa; thoracic tergites with numerous minute and hair-like secondary setae; secondary leg setation detailed in Table 2; CO with 1–2 secondary pores on posterior surface; TR with one secondary pore on proximal portion; LAS with numerous secondary setae, most of them spine-like.

Instar III (Figs 3, 19–23). As second-instar larva except for the following features: Measurements and ratios that characterize the body shape are shown in Table 1. Colour darker; head capsule with one yellow macula around ocularium and another one mesally on frontoclypeus; coxae grey to black over proximal half.

Head (Fig. 19). Apical margin of frontoclypeus with 27–32 spatulate setae. Antenna with A3 shorter than A2. Maxilla with MP2 subequal to slightly shorter than MP1.

Thorax. Spiracles present on mesothorax.

Abdomen (Fig. 20). Spiracles present on segments I–VII.

Table 2. Number and position of secondary setae on the legs of *Platynectes davidorum* sp. nov.

Segment	Position	Instar II (n = 2)	Instar III (n = 3)
Coxa	PD	2–3/2–3/2	2–4/3–4/1–3
	A	0/0–1/2	1–3/2–5/4–7
	Total	2–3–5/2–4/4	5–6/5–8/5–9
Femur	PV	1/1/1	1–2/1/1

Numbers between slash marks refer to pro-, meso- and metathoracic leg, respectively. A = anterior; PD = posterodorsal; PV = posteroventral; Total = total number of secondary setae on the segment (excluding primary setae).

Chaetotaxy. Cephalic capsule with 7–8 spine-like secondary setae on lateral margin and ventral surface of parietale; mandible with several minute secondary setae along outer margin (Fig. 21); secondary leg setation detailed in Table 2 and illustrated in Figs 22–23.

Differential diagnosis. The new species can be easily recognized from any Asian *Platynectes* by dorsally strongly convex habitus, distinctly impressed double reticulation of elytra, and short appendages. In dorsal surface colouration, *P. davidorum* sp. nov. is similar to *P. babai* Satô, 1982 from Taiwan and *P. hainanensis* Nilsson, 1998 from Hainan; however, in addition to characters mentioned above, it is smaller and more roundish. Finally, the new species can readily be distinguished by the shape of median lobe of aedeagus (cf. Šťastný 2003).

In regard to their first instar larva, *Platynectes davidorum* sp. nov. differs from that of *P. curtulus* (the only other *Platynectes* known as first instar) by the following combination of characters: (i) smaller size (HL < 0.6 mm compared to 0.8 mm), (ii) presence of four lamellae clypeales (compared to 10) (Fig. 6), (iii) absence of PV additional setae on femur (Fig. 15), (iv) absence of additional setae on the LAS (Figs 16–17) and (v) the non emarginate posterior margin of the LAS (= siphon) (Fig. 16).

As for the second- and third instar larvae, both *Platynectes davidorum* sp. nov. and *P. curtulus* can readily be distinguished from *P. decemnotatus* by (i) absence of secondary setae on the urogomphus, (ii) a two segmented urogomphus and (iii) the bulge-like appearance of the lateral elongation of the third antennomere (A3') (compared to finger-like). Larvae of *Platynectes davidorum* sp. nov. differ from those of *P. curtulus* by (i) the presence of several tiny secondary setae along the outer margin of the mandible (Fig. 21), a unique feature amongst the known *Platynectes* larvae, and (ii) the absence of dorsal secondary setae on femora (Figs 22–23).

Etymology. The new species is named in honour of four 'Davids': father Armand David (1826–1900), French missionary who collected first reliable material of Chinese beetles; David Sharp (1840–1922), British entomologist who produced a monograph on Dytiscidae and described numerous new taxa from China; David Král, our friend and well known specialist on Scarabaeoidea beetles, who devised the trip to Wuyishan; and last but not least David Hájek, a son of the senior author. The name is a noun in plural genitive case.

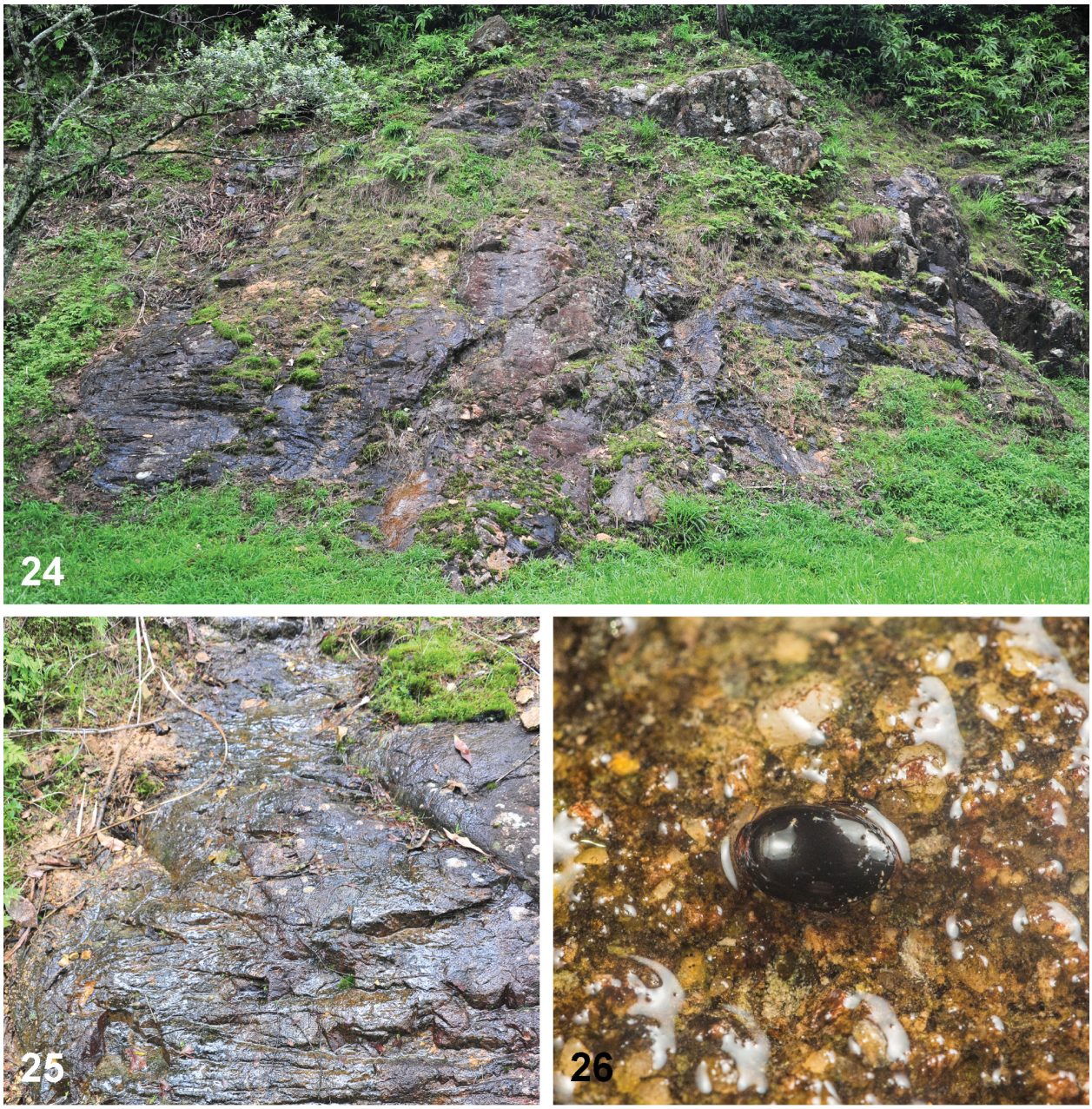

Figs 24–26. Type locality of *Platynectes davidorum* sp. nov. 24 – general view of the habitat; 25 – detail of the microhabitat; 26 – *P. davidorum* sp. nov. in water film on rock surface (photo Yandong Chen).

Collecting circumstances. At the type locality, all adult specimens but one, and all larvae, were collected at night in water film on rock surface of the small cliff (Figs 24–26). One specimen of *P. dissimilis*, a species common in small streams at the locality, was collected together with specimens of *P. davidorum* sp. nov. One female specimen of the new species was collected at light trap.

Distribution. The new species is known so far from two localities in Fujian and Zhejiang Provinces, eastern China, ca. 340 km apart.

Discussion

At the present time *Platynectes* is divided into four subgenera (cf. Nilsson & Hájek 2019). Recent comprehensive molecular phylogenetic analysis of the genus (Toussaint et al. 2017), however, showed that all subgenera except for the Andean *Agametrus* are paraphyletic, which opens to a reconsideration of the actual classification. The subgenus *Gueorguievtes* was proposed by Vazirani (1976) for species with broadly lanceolate prosternal process, metacoxal lines incomplete, and apex of median lobe of aedeagus asymmetrical. Its type species is the Chinese endemic *P. dissimilis*, and as currently defined this subgenus includes all the Oriental, Pacific and the majority of the Australian *Platynectes* species (cf. Nilsson & Hájek 2019). As mentioned above, *Gueorguievtes* is postulated paraphyletic with respect to *Agametrus* and the monotypic Australian subgenus *Australonectes* Guéorguiev, 1972, based on molecular data (Toussaint et al. 2017: 505, Fig. 2). On the contrary the clade comprised of the continental Asian species + Greater Sunda Islands Sumatra and Java

species (clade CIII of Toussaint et al. 2017) is well defined molecularly, and the subgeneric name *Gueorguievtes* in restricted concept is applicable to it. As *Platynectes davidorum* sp. nov. is without any doubts closely related to *P. dissimilis* and *P. gemellatus* (Fig. 24), we herein classify our new species within *Gueorguievtes*.

Platynectes species are found predominantly in lotic habitats such as small streams, springs, or seepages. In Papua and Solomon Islands, some *Platynectes* species were observed to leave streams at night and crawl in wet gravel or even climb small cliff (J. Hájek, unpublished data). Up to now, the only known strictly hygropetric *Platynectes* species was the recently described *P. agallithoplotes* Gustafson, Short & Miller, 2016, collected from seepages on granite outcrops in Venezuela (Gustafson et al. 2016), although several hygropetric *Platynectes* occur also in Australia (L. Hendrich, pers. comm. 2019). Specimens of *Platynectes davidorum* sp. nov. were collected in almost exactly the same habitat as *P. agallithoplotes*. It is worth noting, however, that adaptations for a hygropetric lifestyle seem enhanced in *P. davidorum* as adults of this species are dorsally strongly convex with short appendages, which is unique compared to all known *Platynectes* species. Such habitus is reminiscent of other hygropetric agabine diving beetles such as *Agabus aubei* Perris, 1869 (Balke et al. 1997) and *Hydrotrupes chinensis* Nilsson, 2003 (Alarie et al. 2019). It is worth adding that larvae of *Platynectes davidorum* sp. nov., like those of other species of the genus, are characterized by the almost lack of secondary setae on legs (Figs 22–23). Absence of secondary setae may also indicate an adaptation to a madicolous lifestyle, suggesting that their larvae are not adapted for swimming.

Acknowledgements

We are obliged to Ming Bai (IZCAS) for arrangement of the trip to Wuyishan reserve. Yuanyuan Lu and Yandong Chen (both IZCAS) are thanked for the excellent organisation of the trip in the field. JH would like to thank also David Král (Charles University, Prague, Czech Republic), Jan Růžička (Czech University of Life Sciences, Prague, Czech Republic) and Lukáš Sekerka (NMPC) for their company during the 2018 China trip. We are grateful to Lars Hendrich (Zoologische Staatssammlung München, Germany) and Mariano C. Michat (University of Buenos Aires, Argentina) for valuable comments on the manuscript. The present work was supported by the Ministry of Culture of the Czech Republic (DKRVO 2019-2023/5.I.a, National Museum, 00023272).

References

ALARIE Y. 1995: Primary setae and pores on the legs, the last abdominal segment, and the urogomphi of larvae of Nearctic Colymbetinae (Coleoptera: Adephaga: Dytiscidae) with an analysis of their phylogenetic relationships. *Canadian Entomologist* **127**: 913–943.

ALARIE Y. 1998: Phylogenetic relationships of Nearctic Colymbetinae (Coleoptera: Adephaga: Dytiscidae) based on chaetotaxic and porotaxic analysis of head capsule and appendages of larvae. *Canadian Entomologist* **130**: 803–824.

ALARIE Y. & LARSON D. J. 1998: Larvae of Agabinus Crotch: generic characteristics, description of A. glabrellus (Motschulsky), and comparisons with other genera of the subfamily Colymbetinae (Coleoptera: Adephaga: Dytiscidae). *Coleopterists Bulletin* **52**: 339–350.

ALARIE Y., MICHAT M. C., JIA F. & HÁJEK J. 2019: Hydrotrupes chinensis Nilsson, 2003 (Coleoptera: Dytiscidae): new records, (re) description of adult and larva, and notes on its biology. *Aquatic Insects*, in press. https://doi.org/10.1080/01650424.2019.1601229

ALARIE Y., SPANGLER P. J. & PERKINS P. D. 1998: Study of the larvae of Hydrotrupes palpalis Sharp (Coleoptera: Adephaga, Dytiscidae) with implications for the phylogeny of the Colymbetinae. *Coleopterists Bulletin* **52**: 313–332.

BALKE M., DETTNER K. & HENDRICH L. 1997: Agabus ("Metronectes") aubei Perris: Habitat, morphological adaptations, systematics, evolution, and notes on the phanerofluicolous fauna (Coleoptera: Dytiscidae). *Aquatic Insects* **19**: 75–90.

BENNETI C. J., MICHAT M. C. & ALARIE Y. 2019: Description of the second- and third instar larvae of Platynectes (s. str.) decemnotatus (Aubé, 1838) (Coleoptera: Dytiscidae: Agabinae: Platynectini). *Zootaxa* **4544**: 381–394.

BERTRAND H. 1972: *Larves et nymphes des coléoptères aquatiques du globe.* F. Paillart, Paris, 804 pp.

BEUTEL R. G. 1994: On the systematic position of Hydrotrupes palpalis Sharp (Coleoptera: Dytiscidae). *Aquatic Insects* **16**: 157–164.

GUÉORGUIEV V. B. 1972: Notes sur les Agabini (Coleoptera, Dytiscidae). II. Révision des genres Platynectes Régimbart et Colymbinectes Falk. *Izvestiya na Zoologicheskiya Institut s Muzey Sofia* **34**: 33–62.

GUÉORGUIEV V. B. 1978: Dytiscidae cavernicoles de Papouasie (Résultats zoologiques de la Mission spéléologique britannique en Papouasie-Nouvelle Guinée, 1975, 1). *International Journal of Speleology* **9** [1977–1978]: 267–272.

GUSTAFSON G. T., SHORT A. E. Z. & MILLER K. B. 2016: New species of diving beetles in the subgenus Platynectes s. str. from the Guiana Shield (Coleoptera: Dytiscidae: Agabinae). *Acta Entomologica Musei Nationalis Pragae* **56**: 79–102.

LAWRENCE J. F. 1991: Order Coleoptera. Pp. 144–658. In: STEHR F. W. (ed.): *Immature Insects. Volume 2.* Kendall/Hunt Publishing, Dubuque, 992 pp.

MICHAT M. C., ALARIE Y. & MILLER K. B. 2017: Higher-level phylogeny of diving beetles (Coleoptera: Dytiscidae) based on larval characters. *Systematic Entomology* **42**: 734–767.

MICHAT M. C. & ARCHANGELSKY M. 2009: Phylogenetic relationships of Leuronectes Sharp (Coleoptera: Dytiscidae: Agabinae) based on larval morphology and chaetotaxy. *Insect Systematics and Evolution* **40**: 209–228.

MILLER K. B. & NILSSON A. N. 2003: Homology and terminology: Communicating information about rotated structures in water beetles. *Latissimus* **17**: 1–4.

NILSSON A. N. 1998: Dytiscidae: V. The genus Platynectes Régimbart in China, with a revision of the dissimilis-complex (Coleoptera). Pp. 107–121. In: JÄCH M. A. & JI L. (eds.): *Water beetles of China. Vol. II.* Zoologisch-Botanische Gesellschaft in Österreich and Wiener Coleopterologenverein, Wien, 371 pp.

NILSSON A. N. & HÁJEK J. 2019: *A world catalogue of the family Dytiscidae, or the diving beetles (Coleoptera, Adephaga). Version 1.I.2019.* Distributed as a PDF file via Internet. Available from: http://www.waterbeetles.eu (accessed January 12, 2019)

PETROV P. N., SHAPOVALOV M. I. & FERY H. 2010: A new species of Ilybius Erichson, 1832 (Coleoptera: Dytiscidae) from the North Caucasus. *Russian Entomological Journal* **19**: 41–45.

RATNASINGHNAM S. & HEBERT P. D. N. 2007: BOLD: The Barcode of Life Data System (http://www.barcodinglife.org). *Molecular Ecology Notes* **7**: 355–364.

REMANE A. 1952: *Die Grundlagen des natürlichen Systems, der vergleichenden Anatomie und der Phylogenetik. 1. Theoretische Morphologie und Systematik.* Academische Verlagsgesellschaft Geest und Portig, Leipzig, 400 p.

RIBERA I., VOGLER A. P. & BALKE M. 2008: Phylogeny and diversification of diving beetles (Coleoptera: Dytiscidae). *Cladistics* **24**: 563–590.

ŠŤASTNÝ J. 2003: Review of Platynectes subgen. Gueorguievtes Vazirani from Southeast Asia. Pp. 217–259. In: JÄCH M. A. & JI L. (eds.): *Water beetles of China, Vol. III.* Zoologisch-Botanische

Gesellschaft in Österreich and Wiener Coleopterologenverein, Wien, vi + 572 pp.

ŠUMPICH J. & JAROŠ J. 2019: Chrysoclista karsholti, sp. n., from Turkey, and a new record of C. germanica from central Europe (Lepidoptera: Elachistidae: Parametriotinae). *Zootaxa* **4568**: 587–592.

TOUSSAINT E. F. A., HENDRICH L., HÁJEK J., MICHAT M. C., PANJAITAN R., SHORT A. E. Z. & BALKE M. 2017: Evolution of Pacific Rim diving beetles sheds light on Amphi-Pacific biogeography. *Ecography* **40**: 500–510.

VAZIRANI T. G. 1976: Contributions to the study of aquatic beetles (Coleoptera). 15. Subgeneric classification of Platynectes Régimbart (Dytiscidae). *Records of the Zoological Survey of India* **71**: 169–173.

VONDRÁČEK D., FUCHSOVÁ A., AHRENS D., KRÁL D. & ŠÍPEK P. 2018a: Phylogeography and DNA-based species delimitation provide insight into the taxonomy of the polymorphic rose chafer Protaetia (Potosia) cuprea species complex (Coleoptera: Scarabaeidae: Cetoniinae) in the Western Palearctic. *PLoS ONE* **13(2)(e0192349)**: 1–26. https://doi.org/10.1371/journal.pone.0192349

VONDRÁČEK D., TKOČ M. & FIKÁČEK M. 2018b: Is repeated cypermethrin fumigation dangerous for the mitochondrial DNA in dry insect samples? *Acta Entomologica Musei Nationalis Pragae* **58**: 609–614.

WATTS C. H. S. 1963: The larvae of Australian Dytiscidae. *Transactions of the Royal Society of South Australia* **87**: 23–40.